Journal of the Ceramic Society of Japan 120 [2] 69-73 2012 Paper

Synthesis and characterization of nanometric strontium-doped ceria solid solutions via glycine-nitrate procedure

Branko MATOVIC, Dusan BUCEVAC, Noppasint JIRABORVORNPONGSA,*
Katsumi YOSHIDA* and Toyohiko YANO*,†

Institute of Nuclear Sciences Vinča, Belgrade University, Belgrade 11001, Serbia
***Tokyo Institute of Technology, Research Laboratory for Nuclear Reactors, 2–12–1 O-okayama, Meguro-ku, Tokyo 152–8550, Japan**

Nanometric-sized strontium doped ceria powders were prepared by combustion glycine-nitrate procedure. Cerium nitrate and strontium nitrate were used as starting material whereas glycine is used as a fuel. The tailored composition was: $Ce_{1-x}Sr_xO_{2-\delta}$ with concentration "x" ranging from 0 to 0.15. The effect of dopant concentration and subsequent calcination on crystal stability and lattice parameter was studied. Results showed that the obtained powders were solid solutions with a fluorite-type crystal structure. The particle size was in the nanometric range (<15 nm). Calcination of as-prepared powders at 850°C caused the formation of secondary phase ($SrCeO_3$) in samples containing with fraction of Sr^{2+} ions ≥9 mol %. The solubility limit of Sr^{2+} ions in ceria lattice was between 6 and 9 mol % at 850°C. The solid solution of 6 mol % Sr^{2+} was stable even at temperature as high as 1550°C.

Key-words : Nanopowder, Sr-doped Ceria, Glycine-nitrate procedure, Solid solution, X-ray method

[Received August 29, 2011; Accepted December 9, 2011]

1. Introduction

Cerium dioxide (CeO_2), known as ceria, is technologically important ceramic material. It is frequently used as electrolyte for solid oxide fuel cells, catalyst, oxygen sensor and polishing materials to name a few.[1)–5)] Furthermore, ceria is very important as a model material for studying plutonia properties. Ceria and plutonia have quite similar physicochemical properties such as ionic size in octahedral and cubic coordination, melting point, standard enthalpy of formation and specific heat.[6)–8)] Therefore, the plutonium chemistry could be simulated using ceria instead of highly active PuO_2.[9)] It is worth noting that pure ceria does not undergo phase transformation during heating to high temperature. The room temperature structure, i.e. cubic fluorite structure stays stable up to melting point (~2470°C).[10)] CeO_2 can also make a stable solid solution with many di- and trivalent ions,[11)] which makes it suitable for transmutation host material (inert matrix).[12)–14)] However, the success of many promising technologies is entirely dependent on the development of powder synthesis techniques.[15)] The great variety of methods for nanosized powder synthesis had been published in the literature.[16)–19)] The challenge for these new synthesis techniques is to preserve high powder activity while attaining the desired complex composition. The produced powders must be clean, nanosized, with precise stoichiometry and with homogeneously distributed dopant cations throughout the batch. The applied method should give reproducible powder properties, high yield and must be time and energy effective.

One of the most promising methods to produce a single phase and highly pure nanosized ceria powders with a precise stoichiometry is combustion glycine-nitrate process (GNP).[16),20)–25)] Most of them were synthesis of pure ceria,[20)] gadolinia-doped,[21),23)] samaria-doped ceria[22)] or co-doping of them into ceria.[25)] In this study, the GNP was used to obtain Sr-doped ceria, following our previous study.[25)] Based on these reports, the GNP shows possibility to obtain solid solutions with homogeneous and precise chemistry, and very small particles in tens of nanometer range at very low temperatures. Furthermore, sinterability of obtained powders is superior.[21),23)] According to the literature data Sr-doped ceria powders have not been obtained by this method so far. The effect of dopant concentration on stability of ceria solid solution was examined in order to consider the possibility of using ceria as a host material for storage of radioactive ^{90}Sr isotope.[26)]

2. Experimental

Starting chemicals used for the synthesis of powders were strontium nitrate $Sr(NO_3)_3$, cerium nitrate hexahydrate $[Ce(NO_3)_3{\cdot}6H_2O]$ and glycine (NH_2CH_2COOH) from Wako Chemical Industries, Ltd., Japan. The compositions of the starting reacting mixtures were calculated according to the nominal composition of the final reaction product. The following compositions with varying fraction of Sr substituting for Ce were prepared and the samples were coded as CSX, where X = 3, 6, 9, 12 and 15 mol %.

The applied method for synthesis of ceria solid solutions is glycine nitrate process (GNP). This procedure is based on the exothermicity of the redox reaction between the fuel (glycine) and oxidizer (nitrite). The taken portions of all starting compounds were put into a reactor made of stainless steel, following heat treatment on a hot plate. The burn up process of the reacting liquid mixture was terminated at about 450°C in several minutes. Actually, the procedure needs to be performed in three stages. The first one is dissolution of metal nitrites and glycine in water. The second stage is autoignition of solution at about 180°C which is followed by self sustaining cobmustion giving ash as a product. Finally, the third stage is calcination of ash to burn out organic components in air and obtain pure oxide powder. The reaction could be described as:

† Corresponding author: T. Yano; E-mail: tyano@nr.titech.ac.jp

$$4C_2H_5NO_2 + 2(1-x)Ce(NO_3)_3 \cdot 6H_2O + 2xSr(NO_3)_3 + (2-\delta)O_2 \rightarrow 2Ce_{1-x}Sr_xO_{2-\delta} + (22-12x)H_2O\uparrow + 5N_2\uparrow + 8CO_2\uparrow \quad (1)$$

To determine the crystallite size and lattice parameter of powders both the as-prepared and annealed samples were characterized by X-ray diffraction (XRD) and FE-SEM. XRD patterns were collected using a Simens X-ray Diffractometer (Kristaloflex 500) with Ni-filtered Cu Kα radiation ($\lambda = 0.1541$ nm). The measurements were performed in the range 10 to 80° 2θ in a continuous scan mode with a step width of 0.02° and at a scan rate of 1° 2θ/min. Before measurement the angular correction was done by quality Si standard. The obtained data were fitted using peak-fitting program.[27] The Lorentizian function gave the best fit to the experimental data. The avarage crystallite size of samples, d_{XRD}, was estimated by applying full-width-at-half-maximum (FWHM) of characteristic peak (111) to the Scherrer's equation:

$$d_{XRD} = 0.9\alpha/\mathrm{FWHM} \cdot \cos\theta \quad (2)$$

where α was the incident wavelength (0.15406 nm) of X-ray, and θ was the diffraction angle for the (111) plane. The line broadening caused by instrumentation was corrected. Lattice parameters were refined from the fitted data using the least square procedure. Standard deviation was about 0.001%. Scanning electron microscopy (FE-SEM field-emission type, S-4800, Hitachi, Japan) was used for morphology image of obtained powders.

3. Results and discussions

It is well known that the solubility of different cations into ceria compound depends not only on their ionic radius but also on synthesis method. According to Shannon's compilation,[28] the ionic radii of Ce^{4+} and Sr^{2+} for coordination number 8, are 0.097 and 0.126 nm, respectively. Since Sr^{2+} ion is bigger than Ce^{4+} it is expected that solubility of Sr^{2+} in ceria lattice is low. However, according to X-ray diffraction analysis of as-synthesized powders given in **Fig. 1**, the obtained powders are single phase with fluorite crystal structure. Peaks related to isolated Sr-phases are not observed even in samples containing 15 mol % of the dopant. Relatively high solubility of Sr^{2+} cation into CeO_2 matrix could be attributed to both GNP procedure and nanometric nature of the obtained powders. It is believed that the use of water solutions of nitrates as starting components for GNP provides intimate mixing of Ce and Sr cations, and the result of which is a large amount of Sr cations dissolved into the obtained CeO_2 powder. Moreover, the large amount of gasses created during combustion does not allow excessive growth of newly created nanocrystals of doped CeO_2. It is well known that nanostructured materials are structures far away from thermodynamic equilibrium. This means that they may contain larger number of defects such as Sr^{2+} substitution for Ce^{4+} and therefore accommodate larger amount of Sr^{2+} cations than micron-sized powders. Since nanopowders have short transportation pathways, fast diffusion during calcination often leads to stabilization of powders which in this case causes a decrease in Sr^{2+} solubility. This phenomenon will be discussed later.

The XRD analysis reveals that all peaks for each sample are slightly broadened indicating small crystallite size and/or strain. These XRD patterns were also used to calculate unit cell parameter (a_o). As presented in **Fig. 2**, the unit cell parameter linearly increases with the Sr^{2+} content, which obeys Vegard's law. Clearly, the incorporation of bigger sized Sr^{2+} ions expands the cubic ceria lattice. The calculation based on XRD data shows that the crystallite size of ceria in the as-synthesized powders is below 15 nm for all powders, as the same range of reported crystallite size of 10–25 nm.[20),23),24]

Figure 3 shows XRD patterns of samples with different dopant concentration calcinated at 850°C for 4 h. It can be seen that the peaks are sharper than those recorded for ashes (Fig. 1) indicating the increase in crystallite size after the calcinations. As Fig. 3 evidences the composition with 6 mol % of Sr^{2+} is single phase ceria solid solution. It is important to note that new crystalline phase ($SrCeO_3$) is detected in samples containing more than 9 mol % of the dopant. This indicates that the solid solutions with a large amount of the dopant (≥9 mol %) are not stable at investigated temperature. Despite the presence of secondary phase ($SrCeO_3$) the certain amount of strontium is still dissolved in the ceria lattice. This finding is supported by the fact that the ceria peaks are shifted toward lower angles, which indicates the deformation of lattice due to the incorporation of Sr^{2+} ions. Peak shift with increasing dopant concentration is clearly visible for reflections 331 and 420 (Fig. 3).

As expected, the peak shift is accompanied by the change in lattice parameter. The lattice parameter of doped ceria as a function of Sr^{2+} content for samples calcinated at 600 and 850°C

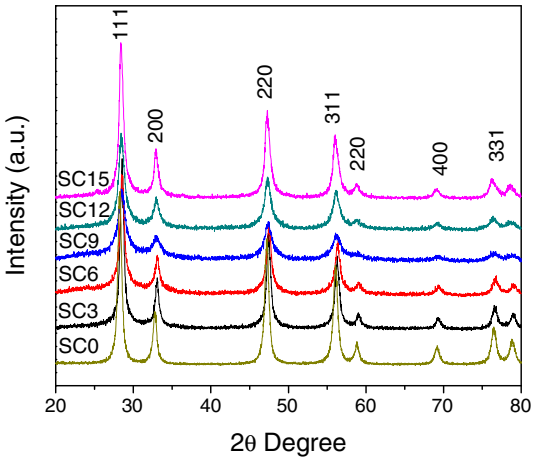

Fig. 1. (Color online) X-ray diffraction patterns of as-synthesized $Ce_{1-x}Sr_xO_{2-\delta}$ powders containing different dopant concentrations (CS0 = 0%, CS3 = 3%, CS6 = 6%, CS9 = 9%, CS12 = 12% and CS15 = 15 mol % of Sr^{2+}).

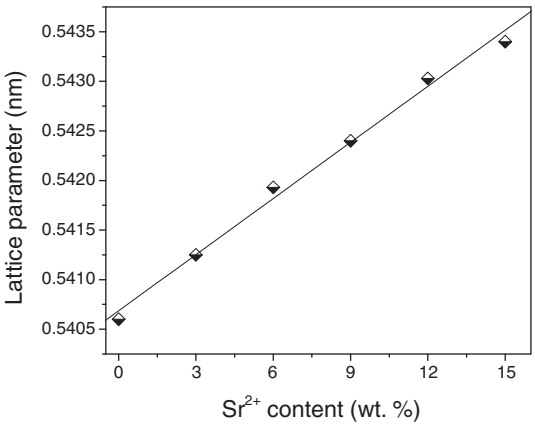

Fig. 2. Lattice parameter (a_o) of as-synthesized $Ce_{1-x}Sr_xO_{2-\delta}$ powders with different Sr^{2+} dopant concentrations.

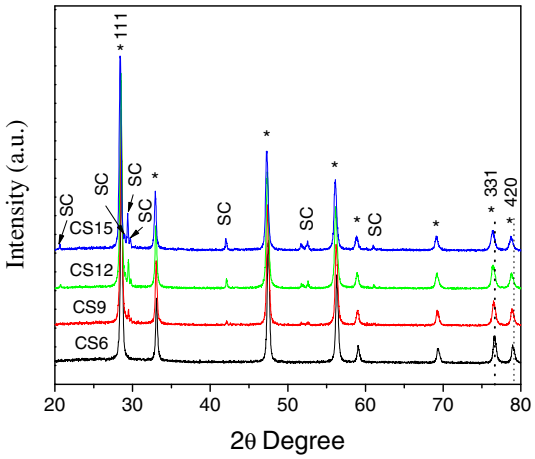

Fig. 3. (Color online) X-ray diffraction patterns of $Ce_{1-x}Sr_xO_{2-\delta}$ powders (CS6 = 6%, CS9 = 9%, CS12 = 12% and CS15 = 15 mol % of Sr^{2+}) calcinated at 850°C for 4 h. (* - CeO_2; SC - $SrCeO_3$).

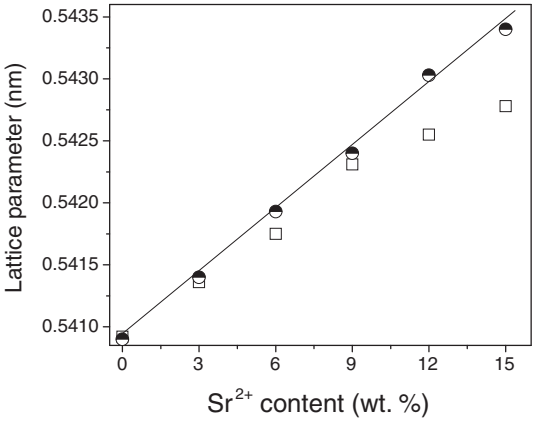

Fig. 4. Lattice parameter of powders with different fraction of Sr^{2+} calcinated at 600°C (half filled circle) and 850°C (square) for 4 h.

is presented in **Fig. 4**. While the lattice parameter of samples calcinated at 600°C obeys Vegard's law, the lattice parameter of samples calcinated at 850°C slightly deviates from linear dependence beyond 9 mol %. This deviation might be attributed to the change of nominal composition due to the segregation of the secondary phase, $SrCeO_3$, at increased temperature. Further support to this conclusion was found in the fact that the lattice parameter of samples calcinated at 600°C is almost the same like that of as-synthesized powders (Fig. 2) whereas the lattice parameter of samples calcinated at 850°C is smaller than that of samples calcinated at 600°C for all Sr^{2+} concentrations except for undoped CeO_2 (Fig. 4). It appears that the increase in calcination temperature promotes rearrangement of structure which results in a decrease in solubility of Sr^{2+} cations in CeO_2 lattice and therefore segregation of $SrCeO_3$ secondary phase.

Now, it would be of interest to calcinate the sample containing 6 mol % Sr^{2+} at higher temperature in order to examine the stability of solid solution. **Figure 5** shows XRD pattern of sample containing 6 mol % Sr^{2+} calcinated at 1550°C for 4 h in air. As can be seen, ceria has fluorite structure even at temperature as high as 1550°C. Since the secondary phase is not observed, it can be concluded that the solubility limit of Sr^{2+} in ceria lattice is more than 6 and less than 9 mol %. The obtained solid solution is stable at high temperature. It is consistent with the report of Yahiro et al,[29] which indicated that the solubility limit of Sr into ceria

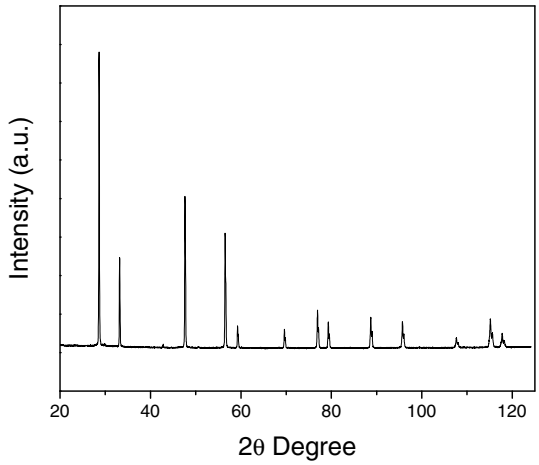

Fig. 5. XRD pattern of $Ce_{0.94}Sr_{0.06}O_{2-\delta}$ sample (CS6) heat-treated at 1550°C for 4 h in air.

was about 8 mol %. In the case of Gd-doped ceria, wide range of solid solubility up to 40% $GdO_{1/2}$ was mentioned,[30] but precise examination showed the stable limit of solid solubility maybe around 20% after sintering at 1550°C, whereas the lattice constant was still increased up to 25%.[31] 20 mol % Sm substitution for Ce was stable after heat-treatment at 1500°C.[24] Relatively small solid solution limit for Sr-dopant can be attributed for the much larger ionic radius of Sr^{2+} (0.126 nm), compared with those of Gd^{3+} (0.105 nm) or Sm^{3+} (0.108 nm).[28]

The microstructures of as-synthesized powder containing 6 mol % Sr^{2+} as well as microstructures of the powder calcinated at different temperature for 4 h in air are presented in **Fig. 6**. The highly porous morphology of as-synthesized powder (ash) [Fig. 6(a)] is the result of large amount of gases created during the combustion, as is the same feature of previous studies.[20)–25)] It can be seen that the ash is open structure consisting of nearly spherical clusters made of clearly visible primary particles. As Fig. 6(b) shows calcination at 600°C destroys skeleton and makes agglomerates of primary particles with less open structure. Furthermore, it is evident from Fig. 6(c) that calcination at 850°C promotes the growth of primary particles and closes the small pores. It seems that very small particle size and therefore high specific surface of ash provides driving force for sintering sufficiently high to initiate sintering at relatively low temperature of 850°C. When calcination temperature is increased to 1550°C the clusters are almost completely sintered. Figure 6(d) shows few small pieces of material attached to fairly smooth surface of much bigger chunk. It is believed that fine powder of doped ceria obtained in this study can be easily sintered at temperature lower than that required for sintering of commercially available powders.

4. Conclusion

Sr-doped ceria solid solutions ($Ce_{1-x}Sr_xO_{2-\delta}$) with "x" ranging from 0 to 0.15 were prepared by glycine-nitrate procedure. It was found that the particle size lies in the nanometric range (<15 nm). Phase identified by XRD was single fluorite and the variation of lattice parameter of the as-synthesized powders (ashes) with increasing Sr^{2+} content obeyed the Vegard's law for full-examined compositional range. The calcination of the as-prepared powders at 850°C caused the formation of a secondary phase ($SrCeO_3$) in samples containing ≥9 mol % Sr^{2+}. The solubility limit of Sr^{2+} ions in the ceria lattice was between 6

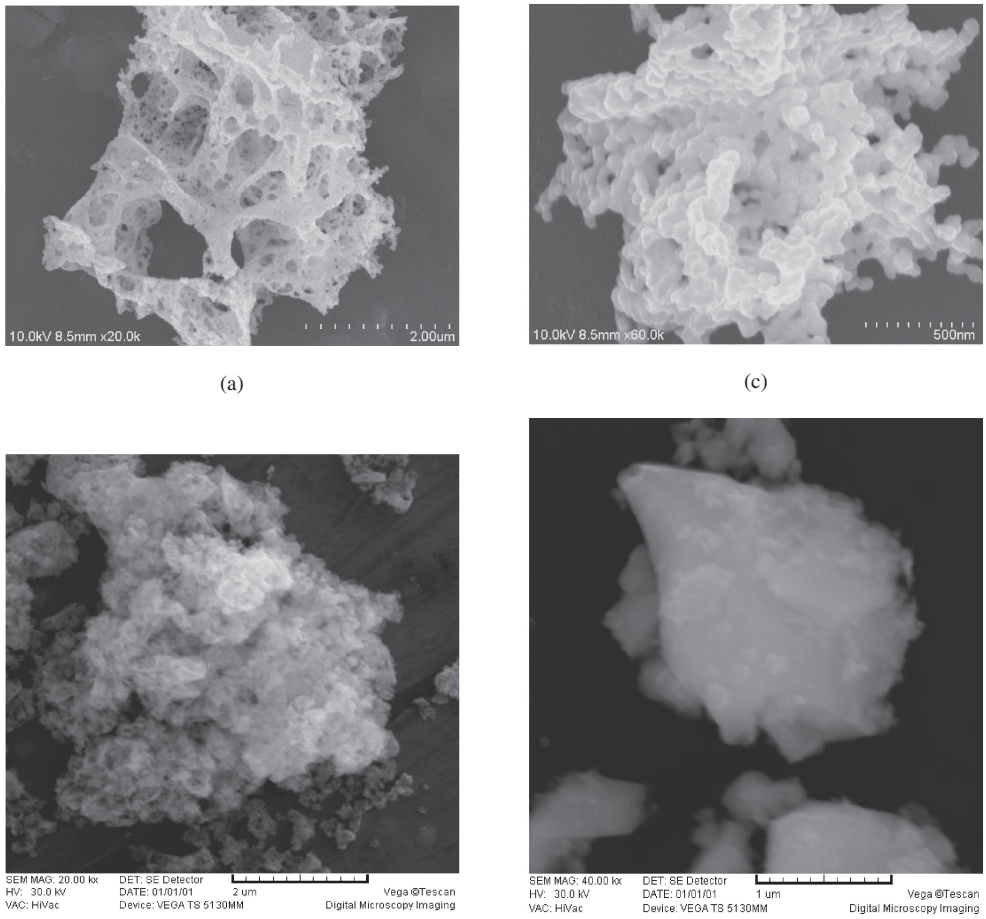

Fig. 6. FE-SEM micrographs of samples containing 6 mol % Sr^{2+}: (a) as-synthesized powder and powders calcinated at b) 600°C, c) 850°C and d) 1550°C for 4 h.

and 9 mol % at 850°C. The stability of 6 mol % solid solution at high temperature was confirmed by heat treatment at 1550°C for 4 h.

Acknowledgements This project was financially supported by the Ministry of Education and Science of Serbia (project number: 45012). One of the authors (Branko Matovic) gratefully acknowledges the financial support from the Tokyo Institute of Technology, Research Laboratory for Nuclear Reactors, 2-12-1, O-okayama, Meguro-ku, Tokyo 152-8550, as a visiting professor.

References

1) H. Inaba and H. Tagawa, *Solid State Ionics*, **83**, 1–16 (1996).
2) S. Boskovic, D. Djurovic, S. Zec, B. Matovic, M. Zinkevich and F. Aldinger, *Ceram. Int.*, **34**, 2001–2006 (2008).
3) P. Dutta, S. Pal, M. S. Seehra, Y. Shi, E. M. Eyring and R. D. Ernst, *Chem. Mater.*, **18**, 5144–5146 (2006).
4) B. Matovic, Z. Dohcevic-Mitrovic, M. Radovic, Z. Brankovic, G. Brankovic, S. Boskovic and Z. Popovic, *J. Power Sources*, **193**, 146–149 (2009).
5) J. Molenda, K. Swierczek and W. Zajac, *J. Power Sources*, **173**, 657–670 (2007).
6) J. C. Mara, A. D. Cozzi, R. A. Pierce, J. M. Pareizs, A. R. Jurgensen and D. M. Missimer, Cerium as a Surrogate in a Plutonium Immobilized Form, in WSRCMS200100007, Contract No. DEAC0996SR18500.
7) H. S. Kim, C. Y. Joung, B. H. Lee, J. Y. Oh, J. H. Koo and P. Heimgartner, *J. Nucl. Mater.*, **378**, 98–104 (2008).
8) R. C. O'Brien, R. M. Ambrosi, N. P. Bannister, S. D. Howe and H. V. Atkinson, *J. Nucl. Mater.*, **393**, 108–113 (2009).
9) M. Burghartz, Hj. Matzke, C. Leger, G. Vambenepe and M. Rome, *J. Alloys Compd.*, **271–273**, 544–548 (1998).
10) C. T. Lynch, in: "High Temperature Oxides", Vol. 5, Ed. by A. M. Alper, Academic Press, New York (1970) p. 193.
11) M. Stojmenovic, S. Boskovic, S. Zec, B. Babic, B. Matovic, Z. Dohcevic-Mitrovic and F. Aldinger, *J. Alloys Compd.*, **507**, 279–285 (2011).
12) K. Choi, W. Tong, R. D. Maiani, D. E. Burkes and Z. A. Munir, *J. Nucl. Mater.*, **404**, 210–216 (2010).
13) R. J. M. Konings, K. Bakker, J. G. Boshoven, H. Hein, M. E. Huntelaar and R. R. van der Lan, *J. Nucl. Mater.*, **274**, 84–90 (1999).
14) G. Szenes, *J. Nucl. Mater.*, **336**, 81–89 (2005).
15) H. Yoshida and T. Inagaki, *J. Alloys Compd.*, **408–412**, 632–636 (2006).
16) S. Boskovic, D. Djurovic, Z. Dohcevic-Mitrovic, Z. Popovic, M. Zinkevich and F. Aldinger, *J. Power Sources*, **145**, 237–242 (2005).
17) S. Boskovic, S. Zec, M. Ninic, J. Dukic, B. Matovic, D. Djurovic and F. Aldinger, *J. Optoelectronic and Advanced Materials*, **10**, 515–519 (2008).
18) T. Zhang, P. Hing, H. Huang and J. Kilner, *J. Eur. Ceram. Soc.*, **21**, 2221–2228 (2001).

19) D. J. Seo, K. O. Ryu, S. B. Park, K. Y. Kim and R.-H. Song, *Mater. Res. Bull.*, 41, 359–366 (2006).
20) R. D. Purohit, B. P. Sharma, K. T. Pillai and A. K. Tyagi, *Mater. Res. Bull.*, 36, 2711–2721 (2001).
21) C. Xia and M. Liu, *Solid State Ionics*, 152–153, 423–430 (2002).
22) D. Xu, X. Liu, D. Wang, G. Yi, Y. Gao, D. Zhang and W. Su, *J. Alloys Compd.*, 429, 292–295 (2007).
23) S. H. Jo, J. H. Kim and D. K. Kim, *Mater. Sci. Forum*, 539–543, 1373–1378 (2007).
24) R. Tian, F. Zhao, F. Chen and C. Xia, *Solid State Ionics*, 192, 580–583 (2011).
25) M. Ninic, S. Boskovic, M. Nenadovic, S. Zec, K. Voisavljevic, D. Minic and B. Matovic, *Sci. Sin.*, 39, 301–308 (2007).
26) K. Yoshida, T. Matsunaga, M. Imai and T. Yano, *J. Ceram. Soc. Japan*, 116, 732–736 (2008).
27) W. Chen, F. Li and J. Yu, *Mater. Lett.*, 60, 57–62 (2006).
28) A. Shannon, *Acta Crystallogr., Sect. A: Cryst. Phys., Diffr., Theor. Gen. Crystallogr.*, 32, 751–767 (1976).
29) H. Yahiro, T. Ohuchi, K. Eguchi and H. Arai, *J. Mater. Sci.*, 23, 1036–1041 (1988).
30) D. J. M. Bevan and E. Summerville, in "Handbook on the Physics and Chemistry of Rare Earths", Ed. by K. A. Gschneider and L. Eyring, North-Holland Physics Publishing, Amsterdam, Oxford, New York, Tokyo (1979) p. 401.
31) Z. Tianshu, P. Hing, H. Huang and J. Kilner, *Solid State Ionics*, 148, 567–573 (2002).